Mausam, (1996), **47**, 4, 369-376

551.510.52 : 551.543

A linear model study of the mid-tropospheric ridge and its displacement

A. CHANDRASEKAR and B. N. GOSWAMI*
Indian Institute of Technology, Kharagpur
(Received 28 December 1994, Modified 30 August 1995)

सार — मध्य क्षोभमंडलीय पर्वत शिखर और उसके विस्थापन की औसत स्थिति की देखभाल के अध्ययन के लिए विलगित ऊष्मा स्रोतों के साथ स्तरित द्रव की स्थायी अवस्था अनुक्रिया वाले एक रैखिक निदर्श का प्रयोग किया गया है। यह स्पष्ट है कि दक्षिण-पश्चिम भारतीय मानसून का 75° पूर्व की ओर अप्रैल 500 एच पी ए पर्वत शिखर की अक्षांशीय स्थिति के साथ घनिष्ठ संबंध है। हाल के प्रेक्षणात्मक अध्ययनों से पता चला है कि यूरेशिया के ऊपर शीत/वसंत हिम आवरण का अप्रैल 500 एच पी ए पर्वत शिखर के साथ नकारात्मक संबंध है। इस अध्ययन में मध्य क्षोभमंडलीय पर्वत शिखर के दक्षिणावर्त विस्थापन की एक व्यवहार्य भौतिक क्रिया विधि का प्रस्ताव रखा गया है। यूरेशिया के हिम आवरण के विस्तार से उत्पन्न असंगत शीतलन उष्णकटिबंधीय ऊष्मा स्रोतों के लिए उत्तर में ऊष्मा अपवाहिका के समान है इससे इस बात का पता चलता है कि ऊष्मा में ऐसी कमी आने के परिणामस्वरूप मध्य क्षोभमंडलीय पर्वत शिखर में महत्वपूर्ण दक्षिणावर्त विस्थापन हो सकता है।

ABSTRACT. A linear model of the steady response of a stratified fluid to isolated heat sources is used to study the maintainence of the mean position of the mid-tropospheric ridge and its displacement. It is well known that the performance of the southwest Indian monsoon is intimately related to the latitudinal position of the April 500 hPa ridge along 75°E. Recent observational studies have demonstrated that the winter/spring snow cover over Eurasia are negatively related to the April 500 hPa ridge position. In this study we propose one possible physical mechanism of southward displacement of the mid-tropospheric ridge. The anomalous cooling associated with the increased snow cover in Eurasia may be considered as a heat sink north of the tropical heat sources. It is demonstrated that such a heat sink can result in significant southward displacement of the mid-tropospheric ridge.

Key words — Mid-tropospheric ridge, Heat sources. Southwest monsoon, Normal modes, Geopotential.

1. Introduction

It is well known that Indian economy is heavily dependent on the performance of the southwest monsoon and hence over the last century, various attempts have been made to evolve methods of predicting the monsoonal rainfall. A review of these attempts is available in the literature (Rao 1965, Shukla 1987, Hasternath and Greischar 1993).

A mid-troposphere ridge pattern over south India and its seasonal migration is a well known feature of the climatology over the Indian region. Earlier studies (Banerjee *et al.* 1978) have shown that if the latitudinal position of the 500 hPa ridge during April is much south (north) of its normal position, rainfall over India for the subsequent summer monsoon is mostly much below (above) normal. The above result is further substantiated by Rao (1981). Mooley *et al.* (1986) have shown that the relationship between the April ridge position and monsoon rainfall over India is highly significant and stable. Verma (1980) examined the monthly mean anomalies of 300-100 hPa thickness, which is a measure of the upper tropospheric temperature anomaly, for 10 years (1968-77) for selected stations over India. Verma found that the anomalies in April and May tend to persist for the whole monsoon season, and that negative (positive) thickness anomalies in the pre-monsoon months are associated with negative (positive) anomalies of Indian summer monsoon rainfall. The long persistence of anomalies in thickness during the months of April and May are more likely to be related to some slowly varying boundary forcing at the earth's surface (Shukla 1987). A strong contender for slowly varying boundary forcing at the earth's surface during the pre-monsoon months is the snow cover over Eurasia.

Blanford (1884) was the first to consider the effect of excessive winter and spring snowfall in the Himalayas on the subsequent monsoon rainfall in India. Hahn and Shukla (1976), after examining 11 years of satellite derived snow cover over Eurasia and summer monsoon rainfall over India, found an inverse relationship between the area extent of winter snow cover over Eurasia and Indian summer

* Indian Institute of Science, Bangalore.

5—168IMD/96

monsoon rainfall. Dey and Bhanukumar (1982) considered the relationship between spring snow cover over Eurasia and the time taken by the Indian summer monsoon rainfall to advance from the southern tip of India to the northern border of India. They found that when the difference of snow cover from March to May was above normal the speed of advance of the monsoon was lower than normal. Bhanukumar [1988 (a & b)] has demonstrated that the satellite derived January snow cover over Eurasia is negatively related to the April 500 hPa ridge position along 75°E and to the Indian monsoon rainfall. The above studies indicate that large and persistent winter snow cover over Eurasia can delay and weaken the spring and summer heating of the land masses, so essential for the establishment of the large scale monsoon flow.

Mooley *et al.* (1986) have advanced the hypothesis that the location of the mid-tropospheric ridge along 75°E is a measure of the influence exerted by the troughs in the westerlies on the upper tropospheric thermal conditions over north and central India. Hence as argued by Mooley *et al.* (1986) a location much south of the normal April ridge location would correspond to a much colder troposphere in April and persistance of colder than normal conditions upto June, which would delay the initiation of monsoonal heat sources, thereby adversely affecting the monsoon.

The latitudinal position of the 500 hPa ridge along 75°E in April has been extensively used by most of the long range forecasters to predict the summer monsoon rainfall since it has emerged as the most powerful of all the predictors (Hasternath and Greischar 1993). Shukla and Mooley (1987) while examining the relationship between the April mid tropospheric ridge location and December through March Eurasian snow cover found a correlation coefficient of −0.49 between the two.

The objective of this study is to propose one possible physical mechanism of southward displacement of the mid-tropospheric ridge. The effect of excessive winter and spring snow cover over Eurasia implies that less solar energy would be available to heat the atmosphere due to high albedo of snow. This can lead to a colder than normal conditions up to June thereby adversely affecting the monsoon. We have demonstrated in this study that a heat sink (corresponding to the anomalous cooling associated with the increased snow cover in Eurasia) prescribed north of one of the heat sources can result in significant southward displacement of the mid-tropospheric ridge.

2. The model

We consider a stratified atmosphere on an equatorial beta plane. Damping is present in the form of Rayleigh friction (α_R) and Newtonian cooling (α_T). The linear equations in log pressure co-ordinates governing steady motion forced by adiabatic heating at a rate Q per unit mass are given by,

$$\alpha_R u - \beta y v = -\frac{\partial \phi}{\partial x} \tag{1}$$

$$\alpha_R v + \beta y u = -\frac{\partial \phi}{\partial y} \tag{2}$$

$$\frac{\partial u}{\partial x} + \frac{\partial v}{\partial y} + \exp(z/H)\frac{\partial}{\partial z}\left[\exp(-z/H)w\right] = 0 \tag{3}$$

$$\alpha_T \frac{\partial \phi}{\partial z} + N^2 w = \frac{R}{H}\left(\frac{Q}{c_p}\right) \tag{4}$$

where, $z = -H \ln (p/p_0)$ and p is the pressure and H is the scale height given by $H = RT_r/g$. The reference pressure and temperature assume the values of 1000 hPa and 300°K providing a scale height of 8.8 km. R is the gas constant and c_p the specific heat at constant pressure. ϕ is the geopotential perturbation and w is the vertical velocity. We assume constant static stability with $N^2 = 1.11 \times 10^{-4} s^{-2}$. The other symbols have their usual meaning. A rigid lid is placed at a height of $D = 22.5$ km above the levels of the forcing (Geisler and Stevens 1982 and Sashegyi and Geisler 1987).

We introduce the variables U, V, Φ such that :

$$(u, v, \phi) = (U, V, \Phi) \exp(z/2H) \tag{5}$$

and eliminate w between (3) and (4) to obtain,

$$\alpha_R U - \beta y V = -\frac{\partial \Phi}{\partial x} \tag{6}$$

$$\alpha_R V + \beta y U = -\frac{\partial \Phi}{\partial y} \tag{7}$$

$$-\left(\alpha_T \Phi\right)\left(\frac{1}{4H^2N^2}\right)+\frac{\alpha_T}{N^2}\frac{\partial^2\Phi}{\partial z^2}$$

$$-\left(\frac{\partial U}{\partial x}+\frac{\partial V}{\partial y}\right)=\frac{1}{\tau}\frac{R}{N^2H^2}F \qquad (8)$$

where,

$$F=-\exp(-z/2H)\left[\frac{Q}{c_p}-H\frac{\partial}{\partial z}\left(\frac{Q}{c_p}\right)\right] \qquad (9)$$

The quantity τ in (8) is the length of the day in seconds and appears as we wish the unit of Q/c_p to be degrees per day.

We define the vertical normal modes as in Geisler and Stevens (1982) by the equation,

$$\left(\frac{d^2}{dz^2}+\frac{N^2}{gh_n}-\frac{1}{4H^2}\right)G_n=0 \qquad (10)$$

and the boundary conditions

$$\left(\frac{d}{dz}+\frac{1}{2H}\right)G_n=0 \qquad (11)$$

at the levels $z=0$ and $z=D$ and $z=D$. Eqn. (11) is due to the fact that the geometric vertical velocity be zero at the top and bottom boundaries.

Expanding the solution variables and the forcing onto the set of vertical modes then gives the equations,

$$\alpha_R U_n-\beta y V_n=-\frac{\partial \Phi_n}{\partial x} \qquad (12)$$

$$\alpha_R V_n+\beta y U_n=-\frac{\partial \Phi_n}{\partial y} \qquad (13)$$

$$\frac{1}{gh_n}(\alpha_T\Phi_n)+\left(\frac{\partial U_n}{\partial x}+\frac{\partial V_n}{\partial y}\right)=\frac{1}{\tau}\left(\frac{R}{H^2N^2}\right)F_n \qquad (14)$$

for the coefficients in this expansion. The coefficient F_n is given by

$$F_n=\frac{\int_0^D F(x,y,z)\,G_n(z)\,dz}{\int_0^D G_n(z)\,G_n(z)\,dz} \qquad (15)$$

The solution of (10) and (11) consists of the external mode

$$G_0(z)=\exp(-z/2H) \qquad (16)$$

and the internal modes

$$G_n(z)=\sin\{(n\pi z/D)-\theta_n\} \qquad (17)$$

where n is a positive integer and

$$\theta_n=\tan^{-1}(2n\pi H/D) \qquad (18)$$

The equivalent depth, h_0 in the case of external mode is infinite, while for the internal modes the equivalent depth is given by

$$h_n=\frac{N^2H^2}{g}\left[\frac{1}{4}+\left(\frac{n\pi H}{D}\right)^2\right]^{-1} \qquad (19)$$

With a depth $D=22.5$ km, the first six internal modes have equivalent depths of 498, 140, 63, 36, 23 and 16 m, respectively.

3. Description of heat sources

The axis of the mid-tropospheric ridge along 75°E as located from the streamline analysis of the average wind data for period 1951-65 by the India Meteorological Department (1972) is seen at about 11.5°N during January, 15°N during April, 28.5°N during July (northernmost location) and 20°N during October (Fig. 2 of Shukla and Mooley 1987). The northward and southward displacement of this mid-tropospheric anticyclonic circulation seems to be related to the seasonal march of the solar radiation and the associated diabatic sources. It is evident that a broken structure of the Inter Tropical Convergent Zone (ITCZ) over the Indian region and its neighbourhood can lead to the mean mid-tropospheric circulation and the associated ridge line as seen in Fig. 2 of Shukla and Mooley (1987). A broken structure of the ITCZ over the Indian region can, in turn, be modelled by prescribing two convective heat sources. In the first part of this study we tried to simulate the mid-tropospheric anticyclone (Fig. 2 of Shukla and Mooley, 1987) by prescribing two non-circular heat sources centered at (0, 1) and (5, 1), respectively. The heating function for a single source is defined as

$$Q(x,y,z)=H(x,y)f(z) \qquad (20)$$

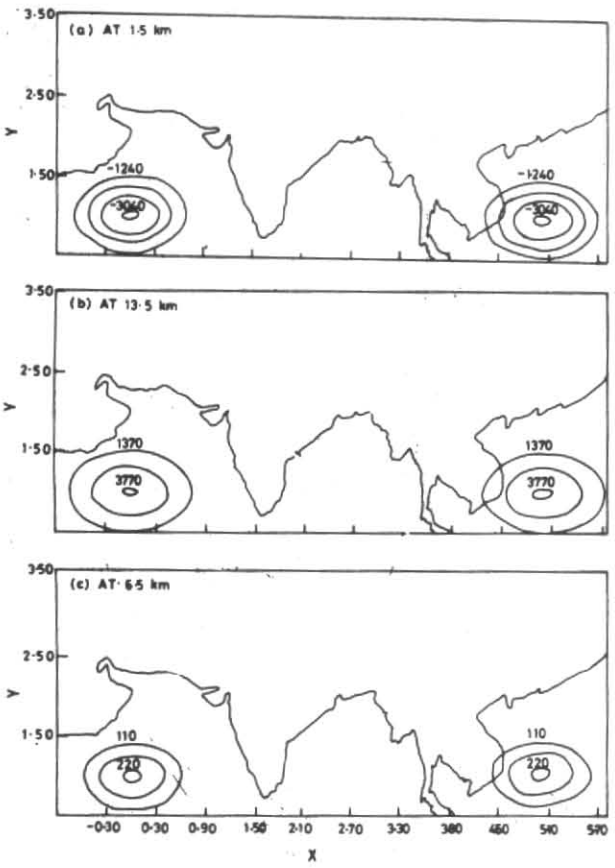

Figs. 1 (a-c). Contours of geoepotential perturbation field (m^2s^{-2}) for two sources at (a) 1.5 km, LC = −3040 and CI = 600, (b) 13.5 km, HC = 3770 and CI = 1200 and (c) 6.5 km, HC = 220 and CI = 55

where,

$$\widetilde{H}(x,y)=\exp[-\alpha_1^2(x-x_0)^2-\alpha_2^2(y-y_0)^2] \qquad (21)$$

where, (x_0, y_0) is the center of the heat source, $\alpha_1^2 = 2$; $\alpha_2^2 = 4$ (the corresponding e — folding distance in x and y direction being 873 and 618 km respectively) and $f(z)$ is defined as,

$$f(z) = \begin{cases} 0 & z \geqslant z_U \\ A \sin(\pi\eta)e^{-b\eta} & z_L < z < z_U \\ 0 & z \leqslant z_L \end{cases} \qquad (22)$$

where, $\eta = (p - p_U)/(p_L - p_U)$ (23)

p_L and p_U were chosen as 1000 and 100 hPa and the corresponding z_L and z_U turned out to be 0 and 20.25 km. b is a parameter which determines the shape of the vertical heating field. $b = 0$ corresponds to a heating field which is symmetric while b positive and b negative correspond to maxima of heating in the upper and lower troposphere. Here, we have used the symmetric heating ($b = 0$). A has been chosen such that $f(z)/c_p$ vertically averaged over the entire atmospheric column corresponds to a heating of 3°C/day.

The equations (12) – (14) are non-dimensionalized by using the length and time scales as follows. $L_1 = (C_1/2\beta)^{1/2}$ and $T_1 = (1/2C_1\beta)^{1/2}$, where, C_1 is the gravity wave speed of the first internal mode, $C_1^2 = gH$, where $H = 498$ m. β is assumed to have a value $2.29 \times 10^{-11} m^{-1}s^{-1}$. The non-dimensionalised steady shallow water equations are solved for each of the first six internal modes and the solution variables are summed over these six modes. The solution procedure is similar to that discussed by Gupta and Manohar (1979). The geopotential is eliminated in the momentum equations using the continuity equation and the following solution procedure adopted :

(a) Start with some approximation for the meridional velocity $v^{(m)}$ with $m = 0$. If no approximation is available set $v^{(m)} = 0$.

(b) Solve u-momentum equation by relaxation method to obtain $u^{(m+1)}$

(c) Determine boundary value of v from u-momentum equation. Call these values $v^{(m+1)}$. Obtain the modified boundary value $v^{(m+1)}$ using a smoothing parameter δ

$$v^{(m+1)} = (1 - \delta)\, v^{(m+1)} + \delta\, v^{(m)} ; 0 < \delta < 1$$

(d) Solve v-momentum equation by relaxation method to obtain $v^{(m+1)}$

(e) Repeat steps (b) to (d) for $m = 1, 2, \ldots$ until convergence criteria is met.

Steps (b) to (d) form outer iterations. For an estimate of δ we determine growth factor ρ of outer iteration

$$\rho = \frac{\| u^{(n+1)} - u^{(n)} \|}{\| u^{(n)} - u^{(n-1)} \|}, \; n \text{ large} \qquad (23a)$$

Norm used is maximum norm, *i.e.*, $\| u \| = | u_{i,j} |$. Knowing ρ the optimal value of δ is found from $\delta = \rho / (\rho + 2)$. Outer iteration were stopped when $\| v^{(n)} - v^{(n-1)} \| < 10^{-4}$. After attaining convergence the geopotential ϕ was obtained from the continuity equation. The domain is rectangular having $-2.5 \leqslant x \leqslant 7.5$ and $-2 \leqslant y \leqslant 5$ with $\Delta x = 0.1$ and

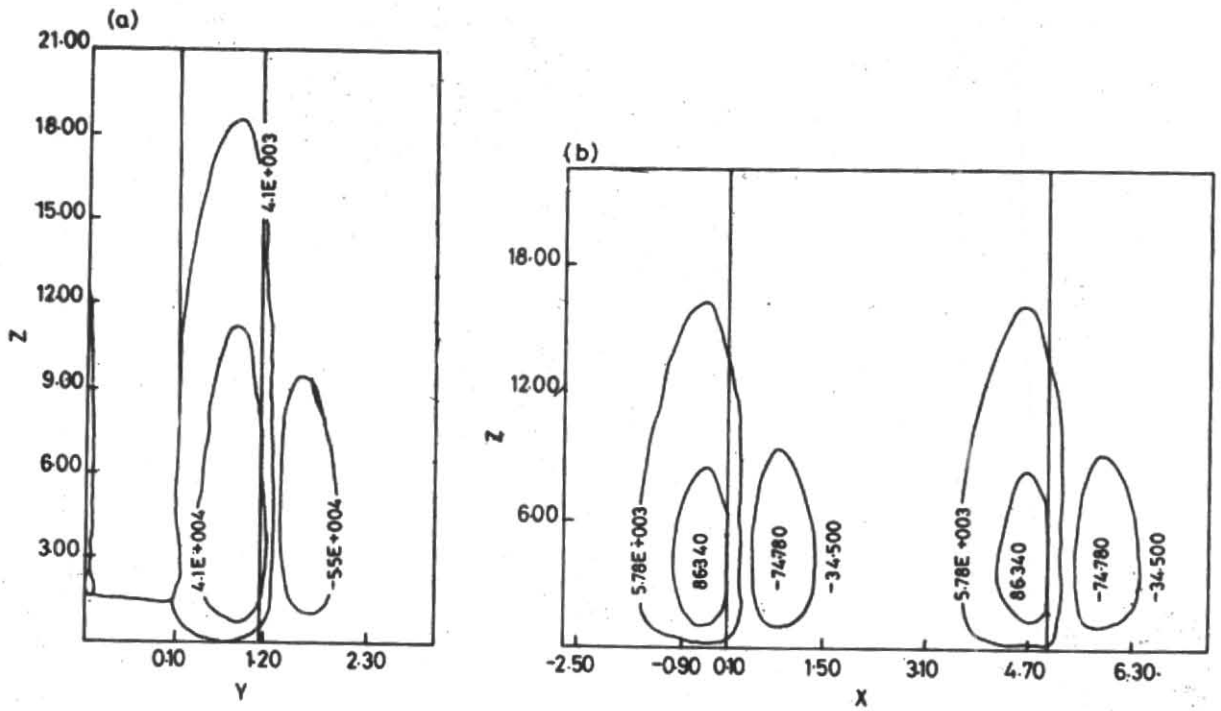

Figs. 2 (a & b). Contours of (a) meridional and (b) zonal mass flux stream function (kg s^{-1}) for two sources

$\Delta y = 0.05$. The values of α_R and α_T are each equal to 0.05. (dissipation time scale being about 4 days) Arakawa *C*-grid is used for horizontal differencing and a Shapiro filter to remove two grid wavelengths is used.

4. Results

4.1. *Experiment 1 : Two noncircular sources centered at (0, 1) and (5, 1)*

Fig. 1 (a) presents the geopotential perturbation field at a height of 1.5 km. Fig. 1 (a) clearly shows a low situated over each of the heating centers. A high of similar structure is seen in the upper Fig. 1 (b) and middle troposphere Fig. 1 (c). It is pertinent to note that the centers of the low and high pressure virtually coincide in Figs. 1 (a) and 1 (c). This is at variance with the real situation where the ridge tilts with height. It is felt that the absence of a mean flow is responsible for the lack of tilt with height.

We now consider the zonal and the meridional overturnings by defining the zonal mass flux stream function as,

$$M(x,z)=L_x\rho_r\int_0^z\int_{-2}^{5}e^{-z/H}u(x,y,z)\,dy\,dz \qquad (24)$$

and the meridional mass flux stream function as

$$M(y,z)=L_y\rho_r\int_0^z\int_{-2.5}^{7.5}e^{-z/H}v(x,y,z)\,dx\,dz \qquad (25)$$

where ρ_r is a reference surface density and L_x and L_y are the domain size in the x and y directions, respectively. The expression for $M(x, z)$ and $M(y, z)$ are similar to Sasheygi and Geisler (1987) except that for the latter the same is defined in spherical coordinates.

Figs. 2 (a & b) show the contours of the meridional and zonal mass flux stream function, respectively. Here the difference in magnitude between any two contours gives the magnitude of the mass transport. The stronger of the two meridional cells is situated to the south of the heating center. It is to be noted that the heating center is located approximately at 11°N latitude. The latitude of heating is indicated by a vertical line in Fig. 2 (a). The zonal mass flux stream function as seen from Fig. 2 (b) shows that the zonal cell west of the heating center is the stronger of the two for both of the heat sources. The magnitudes of the zonal mass flux streamfunction obtained here have the maximum values of the order of $8.6 \times 10^4 \text{kgs}^{-1}$.

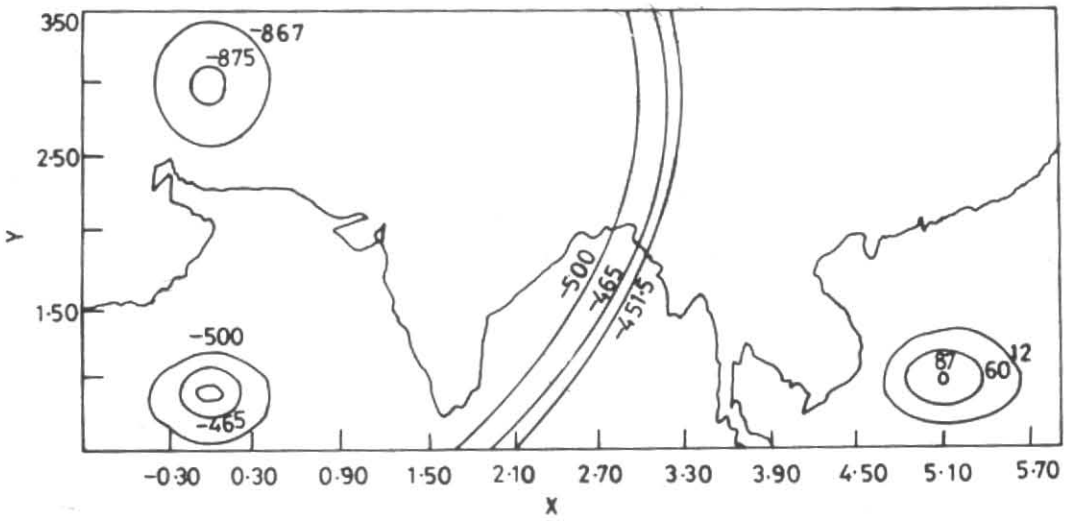

Fig. 3. Contours of geopotential perturbation field (m^2s^{-2}) at 6.5 km for two sources and one sink

4.2. *Experiment 2: Inclusion of a circular heat sink north of one of the heat sources*

In this experiment we have attempted to demonstrate that increased snow cover over Eurasia results in southward displacement of the mid-tropospheric anticyclone. This anomalously cold condition in the north is represented by a circular heat sink north of one of the heat sources of Experiment 1. In order that the heat sink closely resembles the Eurasian snow cover the former is assigned the following characteristics. The sink is quite extensive in horizontal with $\alpha_1^2 = \alpha_2^2 = 0.25$. (e – folding distance of 2470 km) and is centered at (0, 3) roughly at 34°N latitude). We also note that the vertical structure of the heat sink is different from that of the heat sources in the tropics. While the convective sources have maximum heating at the middle troposphere, the sink has maximum cooling in the lower troposphere ($b = -3$) due to enhanced snow cover. The vertically averaged cooling over the entire atmospheric column is assumed to be 2°C/day.

Fig. 3 presents the geopotential perturbation field at a height of 6.5 km after inclusion of the above mentioned circular sink north of one of the heat source. The figure clearly reveals the southward displacement of one of the anticyclones by 123 km (two grid point movement southward). Even though the April mid tropospheric ridge at 75°E is known to experience a maximum southward displacement of about 7° latitude, it is indeed interesting to note that a simple linear model as described above could reproduce a moderate southward displacement. The above model though successful in producing moderate southward displacement of the mid-tropospheric anticyclone has its limitations. Absence of mean wind has been responsible for the absence of tilt with height and hence realistic incorporation of mean winds is imperative. The effect of the advective nonlinear terms may well enhance the southward displacement of the mid-tropospheric anticyclone.

Many investigators have studied the relationship between the winter and spring snow cover over Eurasia and the mid-tropospheric ridge during April along 75°E. They have found that an increased snow cover over Eurasia caused a southward displacement of the mid-tropospheric ridge from its normal position. The effect of excessive snow cover over Eurasia will be that less solar energy will be available to heat the atmosphere due to high albedo of snow. This will invariably lead to a much colder troposphere in April.

While summer conditions begin to be established in the lower troposphere over peninsular India in March, winter circulation prevails over north India until the beginning of May. Due to the southward shift of the extra-tropical westerly belt

in winter, the circulation over north and central India during winter becomes westerly and is periodically influenced by the passage of deep lows or troughs (known locally as western disturbances). In the rear of these disturbances in the westerlies, very cold air from much higher latitudes flows in over north and central India. The ridge demarcates the westerly circulatory regime of the north from the easterly tropical regime to the south. Hence the location of the 500 hPa ridge is a measure of the influence exerted by the troughs in the westerlies on the upper tropospheric thermal conditions over north and central India (Mooley *et al.* 1986). Hence conditions corresponding to a much colder troposphere over north and central India in April should be associated with a marked southward displacement of the 500 hPa ridge. From above, the physical basis for the relationship between the increased snow cover over Eurasia and the latitudinal position of the 500 hPa ridge is clear.

In this study, we have first prescribed two tropical heat sources to simulate the mid-tropospheric circulation over the Indian subcontinent. The heat sources have maximum heating in the mid-troposphere due to release of latent heat of condensation and are not very extensive in the horizontal. The anomalous cooling associated with the increased snow cover in Eurasia is considered as a heat sink north of the tropical heat sources. The heat sink has maximum cooling in the lower troposphere (less solar energy available to heat the atmosphere due to high albedo of snow) due to increased snow cover and is very extensive in the horizontal. Also, we have taken the magnitude of the vertically averaged cooling rate to be less than the vertically averaged heating rate. With the above realistic prescription of heat sources and sink we have demonstrated the feasibility of the physical mechanism of the relationship between the increased snow cover over Eurasia and the latitudinal position of the 500 hPa ridge.

5. Conclusions

A simple linear model of the steady response of a stratified fluid to isolated heat sources is used to study the mid-tropospheric ridge. An attempt has also been made to demonstrate that increased snow cover over Eurasia results in the southward displacement of the mid-tropospheric anticyclone. A circular sink of large horizontal extent and maximum cooling in the lower troposphere is prescribed at 34°N. Inclusion of the above results in moderate displacement of the mid-tropospheric anticyclone by 123 km. We conclude that the model as described above inspite of its simplicity provides encouraging results.

References

Banerjee. A. K., Sen, P. N. and Raman, C. R. V., 1978, "On foreshadowing southwest monsoon rainfall over India with midtropospheric circulation anamoly of April", *Indian J. Met. Geophys.*, **29**, pp. 425-431.

Bhanukumar, O. S. R. U., 1988 a, "Interaction between Eurasian winter snow cover and location of the ridge at the 500 hPa level along 75°E", *J. Meteorol. Soc. Japan*, **66**, pp. 509-514.

Bhanukumar, O. S. R. U., 1988 b, "Eurasian snow cover and seasonal forecast of Indian summer monsoon rainfall", *J. Hydrol. Sci.*, **35**, 5, pp. 515-525.

Blanford, H. F., 1884, "On the connection of the Himalayan snow with dry winds and seasons of droughts in India", Proc. Roy. Soc. London, **37**, pp. 3-22.

Dey, B. and Bhanukumar, O. S. R. U., 1982, "An apparent relationship between Eurasian spring snow cover and advance period of the Indian summer monsoon", *J. Appl. Meteor.*, **21**, pp. 1929-1932.

Geisler, J. C. and Stevens, D. E., 1982, "On the vertical structure of damped steady circulation in the tropics", *Quart. J. R. Met. Soc.*, **108**, pp. 87-93.

Gupta, M. M. and Manohar, R. P., 1979, "Boundary approximations and Accuracy in Viscous flow Computations", *J. Comp. Phys.*, **31**, pp. 265-288.

Hahn, D. and Shukla, J., 1976, "An apparent relationship between European snow cover and Indian monsoon rainfall," *J. Atmos. Sci.*, **33**, pp. 2461-2463.

Hastemath, S. and Greischar, L., 1993, "Changing predictability of Indian monsoon rainfall anomalies?", Proc. Indian Acad. Sci., (Earth & Planet. Sci.), **102**, 1, pp. 35-47.

India Meteorological Department, 1972, "Upper Air Atlas of India and Neighbourhood", Published by India Meteorology Department, New Delhi, 60 maps.

Mooley, D. A., Parthasarathy, B. and Pant, G. B., 1986, "Relationship between Indian summer monsoon rainfall and location of the ridge at the 500 mb level along 75°E", *J. Clim. & Appl. Met.*, **25**, pp. 633-640.

Rao, K. N., 1965, "Seasonal Forecasting—India", Proc. of Symp. on Research and Development Aspects of Long-range Forecasting, Geneva, WMO-IUGG Tech. Note no. 66, WMO-No 162-TP-79, pp. 17-30.

Rao, Y. P., 1981, "The monsoon as reflected in the behaviour of the Tropical High Pressure Belt" in Sir. J. Lighthill and R. P. Pearce, Eds., Monsoon Dynamics, Cambridge University Press, Cambridge, pp. 209-212.

Sashegyi, K. D. and Geisler, J. E., 1987, "A linear model study of cross-equatorial flow forced by summer monsoon heat sources", *J. Atmos. Sci.*, **44**, pp. 1706-1722.

Shukla, J., 1987, "Interannual variability of monsoon", Monsoons, J. S. Fein and P. L. Stephens, Eds., Wiley and Sons.

Shukla, J. and Mooley, D. A., 1987, "Emperical prediction of the summer monsoon rainfall over India", *Mon. Weath. Rev.*, **115**, pp. 695-703.

Verma, R. K., 1980, "Importance of upper tropospheric thermal anomalies for long range forecasting in Indian summer monsoon activity", *Mon. Weath. Rev.*, **108**, pp. 1072-1075.